Discover Applied Sciences

RESEARCH Open Access

Antimicrobial potential and alleviation of arsenic toxicity in human lymphocytes by bacterioruberin and selenium nanoparticles from *Haloferax alexandrinus* GUSF-1 (KF796625)

Jyothi Alvares[1], Sanket Gaonkar[1,2*], Avelyno D'costa[3], S. K. Shyama[3] and Irene Furtado[1]

*Correspondence:
Sanket Gaonkar
micro.sanket@unigoa.ac.in;
prabhugaonkarsanket@unigoa.ac.in
[1]Microbiology Discipline, School of Biological Sciences and Biotechnology, Goa University, Taleigao Plateau, Goa 403206, India
[2]Department of Microbiology, P.E.S's R.S.N College of Arts and Science, Farmagudi, Ponda, Goa 403401, India
[3]Zoology Discipline, School of Biological Sciences and Biotechnology, Goa University, Taleigao Plateau, Goa 403206, India

Abstract

Arsenic contamination is a significant environmental concern indirectly affecting human population. Application of haloarchaea and their biomolecules such as bacterioruberin (BR) and selenium nanoparticles (SeNPs) may play a role in alleviating arsenic toxicity. Considering this, the present study was directed to evaluate antioxidant and antimicrobial properties of SeNPs and BR produced by *Haloferax alexandrinus* GUSF-1 (KF796625) as well as the assessment of interaction of these biomolecules with arsenic to elucidate their possible role in ameliorating arsenic toxicity in human lymphocytes. In addition, study determined the growth behavior and cellular pigmentation pattern of strain GUSF-1 in the presence of arsenic. The results showed the dose-dependent activity of BR and SeNPs against pathogens and more than 50% DPPH radical scavenging activity as well as reduced DNA damage in human lymphocytes associated with arsenic. Interaction of BR and SeNPs with arsenic revealed reduction in intensity and shifts in peak demonstrating the possible interaction of biomolecules and was further confirmed through FTIR. Growth and pigment behavior by GUSF-1 indicated reduced growth and pigmentation in the presence of 5 µM and 10 µM arsenic in complex medium, however showed characteristic peaks with lower intensities corresponding to bacterioruberin. Conclusively, the present findings suggested that, GUSF-1 and its BR and SeNPs will enhance knowledge of the cellular mechanisms underlying the tolerance mechanism to arsenic with a potential for heavy metal bioremediation potential and biomedical applications.

Article highlights

- *Haloferax alexandrinus* GUSF-1 is an haloarchaeon which tolerate As (III) during growth.
- GUSF-1 is a potent producer of bacterioruberin (BR) and selenium nanoparticles (SeNPs).
- BR and SeNPs possess biological activities and ameliorate As (III) toxicity.

Keywords *Haloferax alexandrinus* GUSF-1, Bacterioruberin, SeNPs, Arsenic, Antioxidant, Genotoxicity

1 Introduction

Global data reveals that arsenic contamination has affected over 108 countries, with the highest reports from about 32 Asian countries [1], with southern parts of Asia being highly polluted, including India [2]. WHO recommended 10 µg/L of arsenic in drinking water or 15 µg/Kg intake of inorganic arsenic [3]. Mining rejects from mining activity has been reported to pollute coastal waters worldwide [4]. Mining is the primary contributor to the high concentration of metalloid arsenic in the sediments of the Goan estuarine region of the Zuari and Mandovi rivers [5]. Fondekar and Reddy studied the distribution of inorganic soluble arsenic along the coastal, estuarine, and sea waters of Goa on the West Coast of India [6]. Similarly, a research study by Zingde et al. [7, 8] reported elevated levels of arsenic among crustaceans, causing mortality along the shores of South Goa. Arsenic is classified in group 1 of carcinogenic compounds and is the most significant mass poisoning of the population in history [9].

In humans, inorganic arsenic is reported to interfere with DNA expression and repair [9–12], causing arsenic-induced reactive oxygen damage to various organs [13]. The comet assay is used to study the genotoxicity of inorganic arsenic in human lymphocytes [14–16], wherein DNA damage is monitored by measuring the comet tail length and tail moment. Most studies are reported on using blood cells because they are easy to obtain, and their metabolic state can reflect the overall extent of body exposure to mutagenic and carcinogenic agents. Certain advantages made the comet assay more popular than other genotoxic monitoring platforms, such as micronucleus assay, sister chromatid exchange, and chromosomal aberrations. Comet assay is a versatile, rapid, sensitive, low-cost technology for analyzing and quantifying DNA damage at the cellular level. In addition, the assay requires a small number of cells per sample [17]. Generally, the formation of stress granules (SGs) and a class of proteins called metallothioneins (MTs), enzymatic antioxidants such as reduced glutathione (GSH) and GSH-related enzymes, biomolecules such as jasmonic acid, different antioxidants like L-ascorbic acid and α-tocopherol are reported as cellular responses in the modulation of As-induced oxidative stress [18–22].

In microorganisms, arsenic resistance is usually conferred by several ways. It includes, arsenite and arsenate resistance genes in the genome and mega-plasmid for reduction and oxidation, bioaccumulation of arsenic in the cell, surface adsorption through various functional groups on the cell and biomolecules, the presence of radical scavenging ability of the biomolecules secreted in relation with oxidative stress and biosorption and methylation [23].

Haloarchaea, or halophilic archaea, is a major Euryarcheota group from the domain Archaea. In 2024, Cui and team proposed new members with validly published names under Halobacteria, consisting of nine families, 82 genera, and 351 species [24]. They are widely distributed in highly saline environments, with maximum growth occurring in the presence of 200–350 g/L (w/v) of NaCl [25]. These hypersaline environments are mostly polluted with non-useful toxic oxyanions/heavy metals (Pb, Cd, Hg, As) from anthropogenic activities [26]. The presence of these oxyanions forms an additional stress to the haloarchaea along with fluctuating salinity [27]. Haloarchaea possesses unique physiological and metabolic capabilities. They grow in high concentrations of cations and anions due to their high tolerance and requirements of these elements for growth. In addition, the unique cell structure of haloarchaea, consisting of different cell

envelopes, allows them to tolerate and resist toxic compounds in the environment and high salinity [28, 29]. Interestingly, haloarchaea growing in the presence of toxic metals are reported to synthesize nanoparticles [30] and perform the process of detoxification through their unique metabolic pathways [26, 29, 31–34]. Concerning arsenic, recent study highlighted increase tolerance of haloarchaea to 700 mM arsenic [35]. In other studies, haloarchaea such as *Halorubrum* sp. AD156 and BC156 from Andean Puna [36], *Halorubrum*, *Natronomonas*, *Halonotius*, *Halohasta*, *Natronococcus* and *Halorhabdus* from biofilms of Diamante lake [37] were retrieved which are involved in arsenic bioremediation. *Haloarcula* sp. IRU 1 from hypersaline lake of Urmia accumulate arsenic with 60–89% efficiency at 40 °C, pH 8 and 90 mg/L sodium arsenite [38]. Wang et al. [39] examined genome of *Halobacterium* sp. strain NRC 1 for genes responsible for arsenic resistance.

Recent exploration of haloarchaea and their biomolecules has focused on its potential use in biomedical, industrial, food, wastewater treatment, and bioremediation [25, 40]. Among haloarchaeal metabolites and their applications, using low-toxic carotenoids and nanoparticles in human therapeutics and diagnostic platforms is gaining momentum [40–42].

Haloferax alexandrinus GUSF-1 (KF796625) is a haloarchaeon from a salt pan in Goa-India. It grows optimally at 37 °C and with 25% NaCl. The culture is reported for its numerous bio-prospects, all of which are of industrial and environmental importance. For instance, culture is known to produce wide array of intracellular and extracellular proteins, carotenoids, exopolysaccharides etc. whose role has been exploited in various studies. The strain GUSF-1 is reported to show tolerance to heavy metals [43, 44]. The antioxidant potential of the culture is attributed to the production of characteristic C_{50} carotenoids [45, 46]. Further, the strain is reported for its ability to reduce selenite and tellurite to nanoforms both mediated by the involvement of pigment and soluble intracellular proteins [47, 48]. In addition, the strain showed tolerance to Fe (II) reducing to iron oxide by virtue of iron reductase [49]. Also, biogenic formation of biogenic formation of manganese-based mineral rhodochrosite [50] and Mn_3O_4-MnO_2 nanocomposites [51] are reported. Their study highlighted the involvement of multicopper manganese oxidase for rhodochrosite formation and biomolecules in cell lysate produced by the strain for Mn (II) to Mn_3O_4-MnO_2 nanocomposites. Patil et al. [52] exploited the potential of the strain for the reduction of silver nitrate to silver. They documented the role of carbonyl group corresponding to amino acids and proteins in the biogenic formation and stabilization of nanoparticles.

Over the past decades, efforts have been made to avert and ameliorate cellular damage induced by arsenic using functionalized selenium nanoparticles such as porous Se@SiO_2, chitosan SeNPs, bovine serum albumin SeNPs, starch stabilized SeNPs [53] and plant-mediated selenium nanoparticles [54]. Similarly, natural antioxidants like pigments are known to suppress the toxicity of arsenic by inhibiting the generation of free radicals and oxidative stress during arsenic metabolism in the body [55]. For instance, carotenoids such as β- carotene ameliorate the toxicity of arsenic in albino mice [56].

Considering the necessities to develop an efficient and low-toxic alternative to ameliorates arsenic toxicity affecting the human health and ecosystem, the present study was directed to (i) evaluate the antimicrobial and antioxidant potential of bacterioruberin and selenium nanoparticles produced by *Haloferax alexandrinus* GUSF-1, (ii) assess the

interaction of BR and SeNPs with arsenic (iii) elucidate their possible role in ameliorating arsenic induced DNA damage in human lymphocytes and iii) determine the growth behavior and cellular pigmentation pattern of strain GUSF-1 in the presence of arsenic.

2 Materials and methods

2.1 Chemicals and reagents

Media components, solvents, and chemicals used in the study were of analytical grade and were procured from Himedia laboratories and Sd-fine chemicals (India). A stock solution of 0.1 M sodium arsenite and 0.1 M sodium selenite solution was prepared separately in ultra-pure water (Millipore, Direct Q-3) and filtered by passing through a 0.22 µ nitrocellulose filter. Normal melting point agarose (NMPA) and low melting point agarose (LMPA) were obtained from Sigma Chemical Co. (St. Louis, MO, USA).

2.2 Culture and maintenance

The culture under study, *Haloferax alexandrinus* GUSF-1, was a salt pan isolate with GenBank accession number KF796625. The culture was routinely cultured at 37 °C on NaCl Tryptone Yeast Extract agar (NTYE). The medium consisted of g/L: 20 $MgSO_2.7H_2O$, 5 KCl, 0.2 $CaCl_2.2H_2O$, 5 Tryptone, 3 Yeast Extract, 250 NaCl/solar salt. Solar salt was weighed separately, dissolved in distilled water and filtered using adsorbent cotton. The clear filtered solution was added to the solution containing other medium components. Finally, $CaCl_2.2H_2O$ was added to the medium in dropwise manner to avoid precipitation of the medium during sterilization. The content was uniformly mixed and pH was adjusted to 7.0 ± 0.2 using 1 N NaOH [57].

2.3 Isolation of bacterioruberin (BR) and synthesis of selenium nanoparticles (SeNPs) by *Haloferax alexandrinus* GUSF-1

The culture was grown under optimum conditions in NTYE [45] to extract maximum pigment. After harvesting, the cells were washed with 15% NaCl and treated with methanol in the ratio of 1:1 (cell mass: methanol, w/v). The content was kept undisturbed for 2 h to extract pigment. The mixture was centrifuged at 10000 rpm, 10 min at 4 °C using a high-speed centrifuge (Eppendorf centrifuge 5804 R, Germany. Further, the extraction of BR in methanol was carried out according to Alvares and Furtado [46]. For the production of selenium nanoparticles (SeNPs), *Haloferax alexandrinus* GUSF-1 was cultured in NTYE containing 5 mM/L of selenite, according to Alvares and Furtado [47]. The nanomaterial was harvested from the cells using osmotic shock and washed thrice using Milli Q water. The nanomaterial was then dried in the oven, ground to a fine powder and used for interaction with arsenic to evaluate alleviation of As (III) toxicity in human lymphocytes.

2.4 Antimicrobial activity of BR and SeNps

The antimicrobial activity of BR and biogenic SeNPs to inhibit the growth of pathogenic microbial strains was determined using the procedure of Sahli et al. [58] and Alvares et al. [51], respectively, with some modifications. A stock solution of 1 mg/mL of BR and SeNPs was separately prepared in methanol. Briefly, a loopful of freshly grown pathogenic cultures (*Escherichia coli* ATCC 25922 and *Staphylococcus aureus* ATCC 25923) were inoculated individually in 25 mL of nutrient broth. After 24 h of incubation, 100

µL of each culture was spread plated on the nutrient agar, and the plates were kept for 30 min for adsorption of the pathogens to the surface of the agar. Wells were bored using a sterile 6-mm cork borer. Further, 50 µL of the different concentrations of freshly prepared BR and SeNPs (25, 50, 75, 100, 125, 150, 175, and 200 µg/mL) were added into separate wells. A standard broad-spectrum antibiotic, ciprofloxacin, at 10 µg/mL, and methanol was used as a positive and negative control, respectively. All plates were incubated at 37 °C in the incubator and checked for inhibition of growth after 24 h.

2.5 Evaluation of free radical scavenging activity of BR and SeNps using the DPPH• method

The antioxidant activity of BR and SeNPs was carried out according to Alvares and Furtado [46] with minor modification. A fresh stock solution of 0.1 mM DPPH• reagent (HiMedia) was prepared using methanol. Briefly, 1 mL of different concentrations of BR (25, 50, 100, 300, 500, 700, 900 and 1000 µg/mL) and SeNPs (25, 50, 75, 100, 125, 150, 175 and 200 µg/mL) and was separately reacted with 1 mL of DPPH• solution. The reaction was incubated at 28 ± 2.0 °C in dark. After 30 min, the absorbance of the reaction mixture was measured at 517 nm using a UV-Vis spectrophotometer against methanol as blank. Ascorbic acid (50 µg/mL) (HiMedia) and 0.1 mM DPPH• in methanol were maintained as positive and negative controls, respectively, and were evaluated under similar conditions. The percent DPPH• radical scavenging activity (% DPPH• RSA) by BR and SeNPs was determined using equation.

$$\%\ DPPH\cdot\ radical\ scavenging\ activity = \frac{Absorbance\ (Negative\ Control) - Absorbance\ (Test\ /Positive\ Control)}{Absorbance\ (Negative\ Control)} \times 100$$

2.6 Antigenotoxicity property of BR and SeNps

A 30-year-old whose health status complied with the WHO guidelines for blood donation was considered a donor for human lymphocytes. The blood sample collected in a heparinized tube was centrifuged at 3000 rpm for 15 min. On visual observation, the lymphocytes, which were seen as whitish below the upper plasma layer, were collected, washed with equal volumes of 0.85%, w/v NH_4Cl to remove contaminant RBCs, re-suspended in 0.1 M Phosphate Buffer Saline (PBS), pH 7.4. The viability of the cells was checked by a 0.5% trypan blue exclusion test [59], after which they were adjusted to 10^7 cells/mL using a hemocytometer and stored at 4 °C till further use.

The experimental setup was using a sterile 96-well micro-titre plate. Aliquots of 20 µL of the human lymphocytes were added/ suspended in the first well. A mixture of human lymphocytes with 10 µM of As (III) was added to well number 2. Likewise, human lymphocytes mixed with 10 µM of As (III) and 25 µg/mL of BR or 50 µg/mL of BR or 50 µg/mL of SeNPs made up wells number 3, 4, and 5. Untreated lymphocytes and those suspended in methanol as the negative control were added to wells 6 and 7. After the final volume in each of the wells was made up to 100 µL with 0.1 M PBS pH 7.4, the plate was incubated at 37 °C for two h. The experimental setup was carried out in duplicate.

2.6.1 Assessment of antigenotoxicity by comet assay

The comet assay protocol of Dhawan et al. [60] was used to assess the antigenotoxicity. Under dim light conditions, freshly prepared 400 µl 1% w/v NMPA was poured on a fully frosted glass slide, covered with a coverslip, and allowed to stand at room temperature. After removing the coverslip, separate NMA slides were layered with a mixture of 80 µl

of 0.5% w/v low melting point agarose (LMPA) in 0.1 M PBS, pH 7.4 and 20 µL of either: (i) human lymphocytes; (ii) human lymphocytes exposed to methanol; (iii) human lymphocytes exposed to As (III); (iv) human lymphocytes exposed to As (III) and 25 µg/ mL of BR (v) human lymphocytes exposed to As (III) and 50 µg/ mL of BR (vi) human lymphocytes exposed to As (III) and 50 µg/ mL of SeNPs. A third layer of 100 µL LMPA was added over the second layer and covered with a coverslip. The slides were then placed in freshly prepared, cold lysis solution (2.5 M NaCl, 100 mM EDTA, 10 mM Tris, 10% DMSO, and 1% TritonX-100; pH was adjusted to 10 using 2 N NaOH) in a Petri-dish at 4 °C for 16 h. Each slide was immersed in a horizontal electrophoresis tank containing buffer (300 mM NaOH, 1 mM EDTA, pH 13.5) and allowed to stand for 20 min at room temperature (RT) to enable the unwinding of DNA. Electrophoresis was run at 18 V and 300 mA for 30 min. Each slide was placed in pre-chilled neutralization buffer (0.4 M Tris–HCl, pH 7.5) for 10 min, rinsed with distilled water, and stained with 80 µL of 15 µg/ mL ethidium bromide. A cover slip was placed over the gel on the diffusion of ethidium bromide and viewed using a fluorescence microscope (BX53 Olympus fluorescence microscope-Japan) at 200X magnification and a green filter. Images of individual slides were captured using ProgRes®Capture Pro 2.7. Each captured image was analyzed using CASP image analysis software in Poland for DNA content in terms of its percentage damage [61].

2.7 Interaction of BR and SeNps with arsenic

After successful extraction of BR and SeNPs produced by GUSF-1, the interaction of BR and SeNPs with As (III) was determined separately using UV-visible dual beam spectrophotometer. BR and SeNPs were dissolved in methanol and Milli Q water to prepare 100 µg/mL solution, respectively. Sodium arsenite was dissolved in Milli Q water to achieve 10 µM solution. To study interaction, As (III) and BR/SeNPs were reacted in 1:1 ratio and incubated at RT. After 2 h, the content was scanned in the range of 300–600 nm to monitor any changes in peak patterns and intensity with appropriate solvent as blank using UV-visible dual beam spectrophotometer. For control reaction, BR and SeNPs were incubated in respective solvent in 1:1 ratio under similar conditions and processed as described earlier. Interaction of BR and SeNPs with arsenic in each case was repeated thrice for different time interval to choose the best fit scans demonstrating the interaction.

2.8 Analysis of components associated with BR and SeNps using FTIR

A proof of concept experiment was conducted to ascertain the biocomponents associated with BR and SeNPs responsible for the shift in the plasmon band upon interaction with arsenic. BR and SeNPs were finely ground with KBr separately in the 1:10 (w/w) ratio in this experiment. The KBr-BR and KBr-SeNPs pellets were then scanned in the 4000–400 cm^{-1} range at a resolution of 4 cm^{-1} (IRPrestige-21 Shimadzu). The obtained scans were analyzed for bands corresponding to functional groups associated with BR and SeNPs to unveil the components responsible for interaction with arsenic.

2.9 Growth and pigment production by GUSF-1 in the presence of arsenic

A 5% of freshly grown culture in NTYE was inoculated separately in 100 mL of NTYE with 5 µM and 10 µM of As (III) and without As (III) in 250 mL Erlenmeyer's flask. The

flasks were incubated at 37 °C, under shaker conditions at 120 rpm in a BOD incubator (REMI CIS-24 PLUS, India). Growth of the culture in all three media were monitored daily for period of 8 days as absorbance at 600 nm using a UV-visible dual beam spectrophotometer (Shimadzu-UV 1601, Japan) against an uninoculated medium as a reference solution. Experiments was carried out as three biological replicates to ensure reproducible results and average values were reported with standard error.

Further, the extent of pigment production in the presence and absence of As (III) was monitored to see the effect of arsenic. After 8 days, a fully-grown culture in each broth with and without arsenic was centrifuged and cells were suspended in methanol in 1:1 ratio (w/v). Each cell suspension was sonicated for 5 min cycle and centrifuged at 10,000 rpm, 4 °C for 10 min. The extracted pigment in the supernatant was scanned in the range of 300–600 nm against solvent methanol using UV-visible dual beam spectrophotometer. The difference in spectral scans with respect to shifts in peak and intensity corresponding to bacterioruberin was monitored [57]. Extraction and analysis of pigment in each case was repeated for different period to ensure the reproducibility and the quality of the extracted pigment.

2.10 Statistical analysis

All determinations in the present study was carried out in triplicates and control experiments without arsenic was performed under identical conditions. Results were expressed as mean of three replicate values ± standard error determined using Microsoft Excel. For comet assay, IBM-SPSS 23 software, USA, a one-way analysis of variance (ANOVA) was performed to assess the overall variation in DNA damage and protection to human lymphocytes exposed to 10 µM As (III) (experiment carried out in triplicates). Further, the inter-individual differences between arsenic-induced DNA damage to human lymphocytes and protection by bacterioruberin were compared using Dunnett's multiple comparison test. A level of probability of $p < 0.05$ was considered statistically significant data.

3 Results and discussion

Globally, heavy metal/oxyanion pollution has increased widely, resulting in environmental and human health-associated problems. These contaminations are reported to severely affect the marine environments, including the highly saline econiches. The contaminants primarily included are heavy metals /oxyanions like Cd, Hg, As, Cr, Cu, Zn, Fe, Ni, etc. Among these, Pb, Cd, and Hg do not exhibit any biological role and cause oxidative stress [28, 34]. Compared to conventional chemical methods for removing toxic pollutants, biological approaches possess several advantages, such as being biocompatible and non-toxic, transforming toxic heavy metals, and simultaneously producing nanoparticles. Arsenic contamination is a widespread global issue; documented for human toxicity at low concentrations, besides affecting microorganisms' cellular growth and metabolism [34]. Over a past decade, arsenic bioremediation using microorganisms have been highlighted in various studies [23].

Although there exist studies on carotenoids characterization and their biological properties from haloarchaea [41], few reports are available on the synthesis of nanoparticles of silver [52, 62], selenium [47, 62–64], tellurium [48], manganese [50, 51], and iron [49]. Further, only one study has been carried out on the antioxidant activity of SeNPs

produced by haloarchaea [64], and only one report on the antimicrobial properties of SeNPs against human pathogens [62].

Previously, Alvares and Furtado [46] cultured GUSF-1 in 5 L of NTYE to produce pigment and analyzed the multiple components that comprised the total pigment in the cell. In their study, 107 g of cell biomass is recovered and used to study the multi-components with bioactive potential. In another study, the biological production of SeNPS from GUSF-1 is investigated with the capacity to modulate calcium oxalate crystals [47]. Therefore, the current research aimed to evaluate the bioremediation potential of strain GUSF-1 achieved via its multi-component pigment and SeNPs and to determine their role in ameliorating arsenic toxicity, while also evaluating the antimicrobial and antioxidant features.

3.1 Isolation of BR and synthesis of SeNps

The culture grew with an orange pigment in 1 L of NTYE broth (Fig. S1), producing 20 g of wet cells. The pigment (BR) extracted from the wet cells, weighed approximately 10 mg/L and was stored in a vial at 4° C wrapped in aluminum foil. Selenium nanoparticles production was achieved during the growth of the culture in 5 mM sodium selenite (containing 0.394 g/L of selenite) visible as brick-red particulate matter after 7 days (Fig. S2). Cell lysis of the cell biomass resulted in a total of 0.22 g of SeNPs, which was washed with Milli - Q water, oven-dried, ground to a fine powder, and used for further studies. In our previous study, SeNPs produced by GUSF-1 was characterized in detail using various spectroscopic and microscopic techniques. Transmission electron microscopy showed crystalline pentagonal nanoforms of average size of 11.6 nm. The X-ray diffraction and Energy disruptive analysis of X-ray highlighted peaks indicative of selenium. Further, SeNPs are used to modulate calcium oxalate crystals.

3.2 Antibacterial activity of bacterioruberin and selenium nanoparticles

The antimicrobial activity of BR and SeNPs was estimated using an agar-well diffusion assay. The results revealed that bacterioruberin and selenium nanoparticles produced by *Haloferax alexandrinus* GUSF-1 showed promising antibacterial activity against *E. coli* ATCC 25,922 and *S. aureus* ATCC 25,923 (Fig. 1; Fig. S3). However, relatively lesser inhibition zones were observed in the 13–20 mm range. Abdollahnia et al. [62] observed moderate antibacterial activity for selenium and silver nanoparticles produced by halophilic archaea and bacteria due to the extreme nature of nanoparticles where their capping agents is not involved in increasing the antimicrobial activity as reported for biogenic nanoparticles produced by non-extremophiles. They documented smaller size, low polydispersity index, and high stability of archaeal-based SeNPs that is responsible for antibacterial activity. Sahli et al. [58] reported the antimicrobial activity of carotenoids from *Halorubrum* sp. BS2 against *S. aureus*, *E. coli*, *P. aeruginosa*, and *K. pneumonia* in the 13–15 mm range. Likewise, *Haloferax* sp. ME16 carotenoids displayed antibacterial activity against human and fish pathogenic strains evaluated by the agar disk diffusion method [65]. The antimicrobial activity of bacterioruberin and SeNPs is attributed to either of the proposed mechanism. SeNPs and BR can interact with the functional groups associated with microbial proteins and enzymes, altering their structures. They can block the membrane transport of ions and nutrients through the cells and inhibit metabolic pathways. They can deplete cellular ATP and disturb the

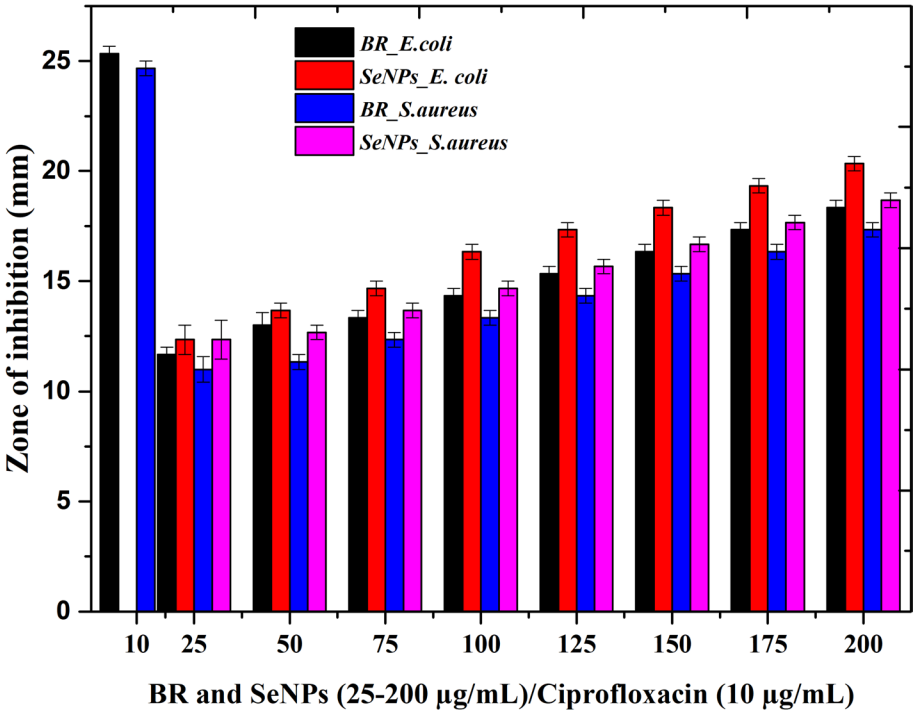

Fig. 1 Antimicrobial activity of BR and SeNPs against *E. coli* ATCC 25,922 and *S. aureus* ATCC 25,923

membrane potential, inhibiting microbial growth. Other reasons may be the inhibition of dehydrogenase activity and cell integrity destruction, inhibition to form microbial biofilm, and catalytic action against the bacteria [65, 66].

3.3 Antioxidant activity of BR and SeNps

DPPH• is widely used to determine antioxidants' free radical scavenging abilities because it acts as a stable free radical donor. The scavenging activity of carotenoids involves electron transfer from the carotenoid to the DPPH•, generating a radical cation attached to the carotenoid [67]. The present study determines the abilities of bacterioruberin and SeNPs synthesized by GUSF-1 to scavenge DPPH•. It was found that, with an increase in the bacterioruberin concentration, there is an increase in the trend for DPPH• RSA. The effect was dose-dependent with a maximum of 83.36 ± 0.30% DPPH• RSA at 1000 µg/mL concentration of bacterioruberin (Fig. 2a, Fig. S4a). The purified BR from GUSF-1 exhibited 80% ± 0.32% DPPH• RSA at 1000 µg/mL [46]. Hou and Cui [68] analyzed the antioxidant potential of carotenoid extracts from different haloarchaea, such as *Hfx. volcanii*, *Hgn. rubrum*, *Hpl. inordinate*, *Hgm. rufum*, *Hgm. limi*, *Hpn. vescus*, and *Hap. litoreus*. Specifically, carotenoids from *Haloferax* sp. ME16 displayed maximum antioxidant activity compared to standard ascorbic acid [65]. Similarly, predominant carotenoids such as bacterioruberin and bisanhydrobacterioruberin from *Halorubrum* sp. BS2 possessed 99% DPPH radical scavenging activity higher than ascorbic acid [58]. A recent report by Nagar et al. [69] documented the antioxidant activity of pigment extracts rich in C_{50} carotenoids and bacterioruberin (BR) derivatives from *Haloarcula* sp. E2 and *Halorubrum* sp. M5 in the 67–70% range between 100 and 400 µg/mL concentration. Bouhamed et al. [70] reported high antioxidant activity of bacterioruberin extracted from *H. salinarum* across four oxidizing assays. At 400 µg/mL concentration,

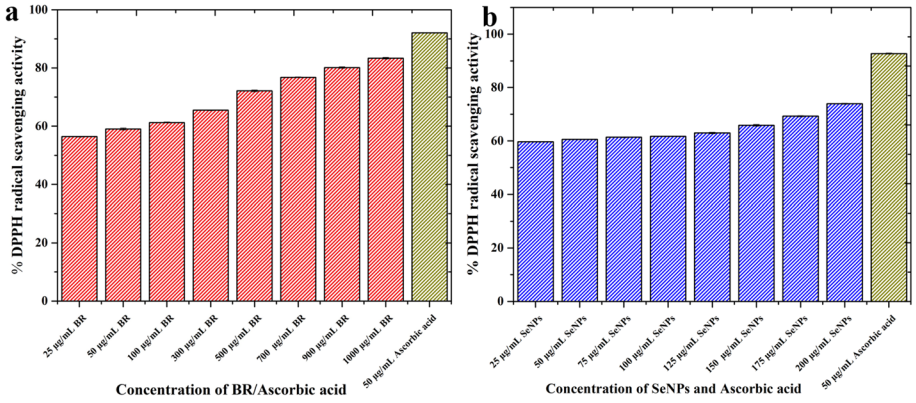

Fig. 2 Antioxidant activity of BR (**a**) and SeNPs (**b**) using DPPH radical scavenging assay. Each antioxidant activity of BR and SeNPs were performed in triplicates at a given time and repeated thrice independently and used for EC50 determination

carotenoid exhibited 89.65% DPPH radical scavenging activity. The structure of bacterioruberin displays extensive 13 conjugated double bond system with two acyclic phi ϕ end groups and four OH. All these three characteristics of bacterioruberin, such as the length, conjugated double bonds, and functional groups, contribute to the antioxidant capacity [41, 46, 69].

The SeNPs showed a similar trend of increasing scavenging activity with increased nanoparticle concentration. A maximum of 73.9 ± 0.20% $DPPH^{\bullet}$ RSA was detected for 200 µg/ mL of SeNPs (Fig. 2b; Fig. S4b). Overall, the DPPH radical scavenging activity of SeNPs was higher than BR at the same concentrations. As reported by Nagar et al. [64], pigment and other biomolecules in haloarchaea are involved in the capping of the nanoparticles may synergistically enhance the antioxidant activity of the SeNPs. In their study, SeNPs produced by genera *Haloferax*, *Haloarcula*, and *Halogeometricum* exhibited 70.5%, 70.3%, and 71.5% DPPH radical scavenging activity, respectively [64]. Further, the EC_{50} concentration values for BR and SeNPs were found to be 18 ± 10 µg/mL and 10 ± 6.0 µg/mL, respectively (Fig. S5a) comparable to the EC_{50} value of standard ascorbic acid reported previously [45]. High standard deviation for EC50 values for DPPH radical scavenging activity indicates that a wide range of BR and SeNPs concentrations may be required to achieve 50% reduction in DPPH free radicals suggesting significant variability. This might be due to heterogeneity in BR and SeNPs composition due to associated proteins, enzymes and ions during the synthesis that may require further purification of antioxidant molecules. This further need attention to validate antioxidant potency of BR and SeNPs for their future possible use in biomedicine. Fig. S5b–g denotes the dose dependent curves for the percentage DPPH radical scavenging activity plotted against $\log_{10}$ [BR/SeNPs] concentration. These dose-response curves were plotted for each triplicate and used for determination of EC50 values. Furthermore, low EC50 values for BR and SeNPs beyond the concentrations depicted in Fig. 2b signifies the ability of the molecules to enhance antioxidant activity at lower concentrations. This was supported by the Fig. S5h & i, wherein, lower concentration of BR and SeNPs showed DPPH radical scavenging activity. However, at these concentrations, the antioxidant percentages were relatively similar for 5, 10, 15 and 20 µg/mL of BR and SeNPs.

3.4 Amelioration of arsenic toxicity on human lymphocytes by BR and SeNps

The human lymphocytes used in the experiment were 90% viable in the trypan blue exclusion test. When viewed under a fluorescent microscope, these human lymphocytes and those exposed to methanol showed intact DNA (Fig. 3A-B; Fig. S6A-B). On exposure of human lymphocytes to 10 µM As (III) for 2 h, the human lymphocyte number was reduced to 65% with the appearance of comet-like images in the ethidium bromide-stained slides (Fig. 3C; Fig. S6C). The mean % tail DNA of these comet-like images was 82.43% ± 9.57. Such damage was related to strand breaks, which cause fluorescence to spread, indicating the genotoxic effect of 10 µM As (III) resulting in DNA strand breaks consistent with that reported by Kumaravel et al. [71] and Lee and Weinfeld [20].

Interestingly, the addition of 25 µg/mL, 50 µg/mL of BR, and 50 µg/mL SeNPs during exposure of human lymphocytes to As (III) reduced the adverse effect of As (III) on the viability of human lymphocytes up to 76%, with an accompanying decrease in the DNA damage by 68% (mean % tail DNA of 26.06% ± 10.58); an additional 24% (mean % tail DNA of 6.196 ± 2.80) and 42% (mean %tail DNA of 47.84 ± 0.823) respectively (Fig. 3D–F; Fig. S6D–F).

Further, as seen in Fig. 4, the statistical analysis: one-way ANOVA and Dunnett's multi-comparison revealed that BR enhanced dose-dependent protection to human lymphocytes with a highly significant variation of $F = 43.666$; $p < 0.001$. The Cell suspension of *H. salinarium* containing bacterioruberin has been reported to reduce DNA strand breaks resulting from ionizing radiation, UV, Hydrogen peroxide, and mitomycin-C [72].

The DNA damage by Arsenic was alleviated when As (III) treated cells were mixed with BR and SeNPs. In addition, the lymphocyte cell viability was increased with

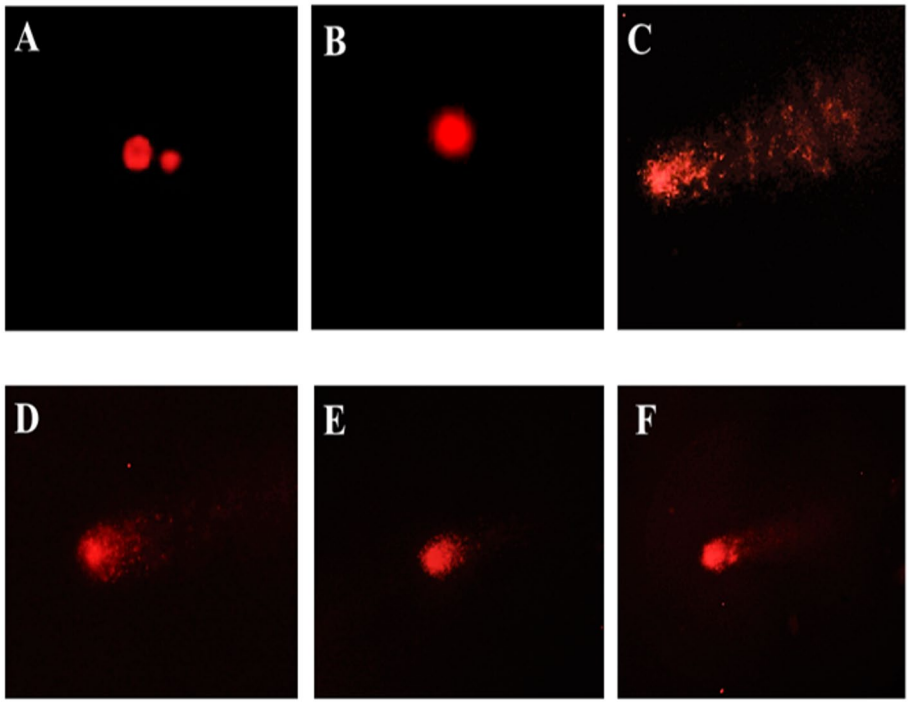

Fig. 3 Fluorescent micrographs of ethidium bromide-stained agarose slides of human lymphocytes (HL) exposed to As (III), bacterioruberin, and selenium nanoparticles. **A** Human lymphocytes (HL); **B** HL exposed to methanol; **C** HL exposed to 10 µM As (III); **D** HL exposed to 10 µM As (III) and 25 µg/mL of BR; **E** HL exposed to 10 µM As (III) and 50 µg/mL of BR; and **F** HL exposed to 10 µM As (III) and 50 µg/mL of SeNPs

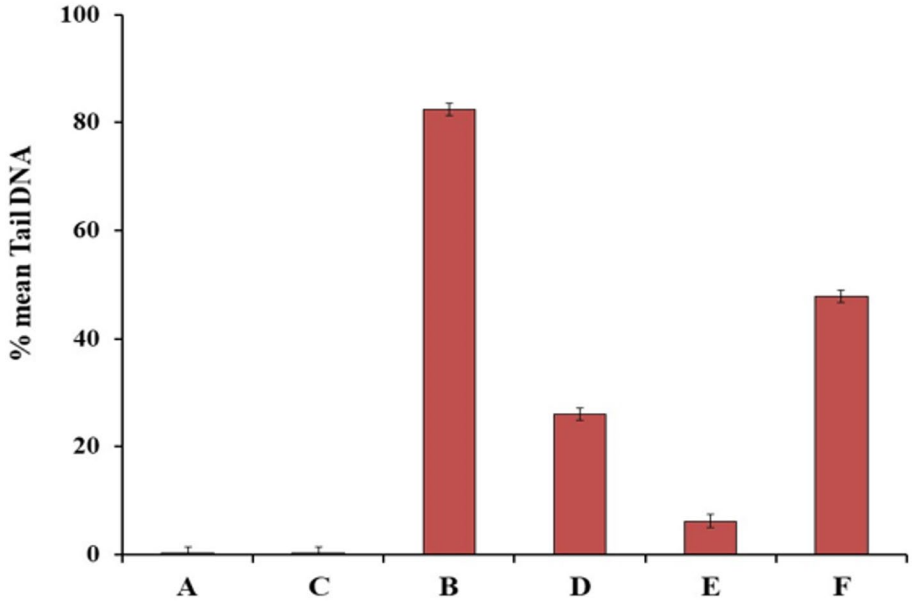

Fig. 4 Suppression of DNA damage caused by As (III) using bacterioruberin and selenium nanoparticles (The DNA damage was evaluated by comet assay and expressed as % mean tail DNA). **A** Human lymphocytes (HL); **B** HL exposed to methanol; **C** HL exposed to 10 µM As (III); **D** HL exposed to 10 µM As (III) and 25 µg/mL of bacterioruberin; **E** HL exposed to 10 µM As (III) and 50 µg/mL of BR; and **F** HL exposed to 10 µM As (III) and 50 µg/mL of SeNPs

decreased DNA tail damage in the presence of BR and SeNPs. The above observation highlights the antioxidant power of both the molecules produced by GUSF-1 in the present study. It might be due to the role of BR and SeNPs in an antioxidant network and the sequestration of free radicals generated by the intoxication of As (III) in cells. Previous studies are reported at the cellular level to confirm the potential of various forms of selenium to alleviate arsenic toxicity [73]. For instance, 0.01 µg/mL of plant-derived SeNPs alleviated arsenite toxicity in cultured human lymphocytes [54]. Their study employed a comet assay to assess the protection rendered by SeNPs towards arsenite-targeted DNA damage. Chitta et al. [74] used selenomethionine to protect arsenite-affected human kidney cells. In another study, Rahman et al. [75] reported the property of inorganic selenium to induce anti-autophagic, anti-apoptotic, and antioxidant properties in arsenite-treated PC12 cells. Recently, the biocompatible ability of SeNPs against sodium arsenite-exposed mice renal tissues and epithelial cells has been highlighted [53]. Together, reduced arsenic toxicity by SeNPs is related to the sequestration of arsenic into biologically inert complexes (As-Se complexes) and the action of selenium-dependent antioxidant enzymes. Also, SeNPs can increase arsenic methylation efficiency and activate signaling pathways [73].

3.5 Interaction of BR and SeNps with arsenic

The interaction of BR and SeNPs with arsenic was studied to ascertain the probable mechanism for transformation to less toxic arsenic. The characteristic peaks and intensity of haloarchaeal pigment in methanol corresponding to 368 nm, 386 nm, 463 nm, 492 nm and 525 nm were shifted and decreased upon 1:1 interaction of BR with 10 µM As (III) (Fig. 5A). A remarkable hypsochromic shift from 386 to 380 nm and 368 to 360 were also observed upon interaction or adsorption of As (III) ions with BR. In addition, the peak intensity at 463, 492, and 525 nm of BR was decreased to 65.8%, 64.2%,

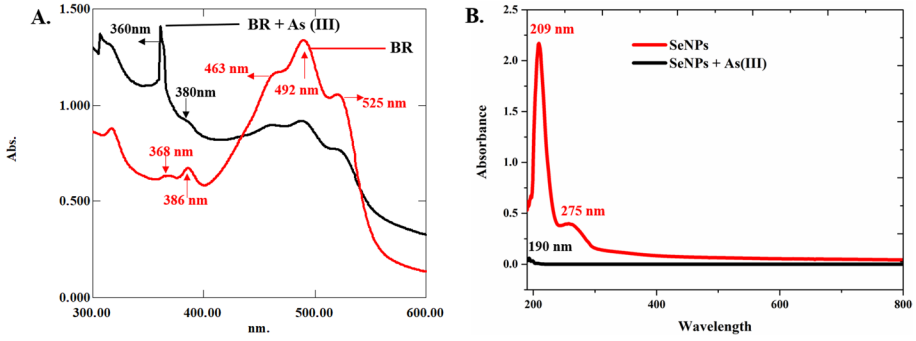

Fig. 5 Interaction of BR and SeNPs with As (III). **A**, Spectrophotometric scan of BR and BR with 10 µM of As (III); **B**, Spectrophotometric scan of SeNPs and SeNPs with 10 µM of As (III)

and 63.3%, respectively, suggesting its direct involvement in the detoxification process. On the other hand, the peak and the intensity of the spectrophotometric peak which was characteristic of SeNPs at 209 nm was shifted to 190 nm with an additional peak at 275 nm was abolished after interaction with As (III) (Fig. 5B). This confirms the probable interaction of surface-modified SeNPs with the arsenic ions. The strong interaction between arsenic and selenium metalloids could be due to their similar chemical properties, although they exhibit different biological activities [61]. Overall, the present study hypothesized following proposed mechanisms for As (III) interaction with BR or SeNPs. The first case is attributed to the ionic interaction of As (III) with BR/SeNPs and adsorption of As (III) on the surface of the SeNPs. Concerning specifically BR, it consists of long hydrocarbon chain with higher number of double bonds in conjugated form than other carotenoids responsible for extraordinary antioxidant activity [35, 41]. In addition, the presence of electron transport system between conjugated double bonds may be involved in transfer of electrons that can interact with As (III) thereby reducing it to elemental arsenic [As (0)]. SeNPs may allow adsorption of arsenic through capping agents preventing its accumulation inside the cell thereby activating superoxide dismutase, glutathione peroxidase and thioredoxin reductase neutralizing the free radicals and thus oxidative stress caused by arsenic. Understanding theses hypothetical mechanisms of BR and SeNPs could inspire for the development of therapies targeting heavy metal oxidative stress induced DNA damage reported previously offering applications in biomedicines.

3.6 Analysis of components of BR and biomolecules associated with SeNps using FTIR

A proof of concept experiment using FTIR was conducted to ascertain the role of individual components of bacterioruberin and biomolecules associated with SeNPs that could be essential in interaction with As (III). The FTIR spectrum of BR (Fig. 6a) revealed the absorption bands between 3300 and 500 cm^{-1}. Intense absorption bands were seen at 3302 cm^{-1} for the OH group. The band at 2954 cm^{-1} indicated the presence of the C–H group, and at 1624 cm^{-1} for the carbonyl group. Absorption bands were also seen at 1573 and 1022 cm^{-1}, which means the C–OH side groups and the C–O–C band vibrations. In addition, CH_3 bending was observed at 1444 cm^{-1} and 1379 cm^{-1}. Also, a band at 879 cm^{-1} was observed, corresponding to C–H bending. Alvares and Furtado [46] reported similar assigned bands for pigment extract from GUSF-1. Later, chemical profiling of the hexanolic extract of pigment from GUSF-1 confirmed the

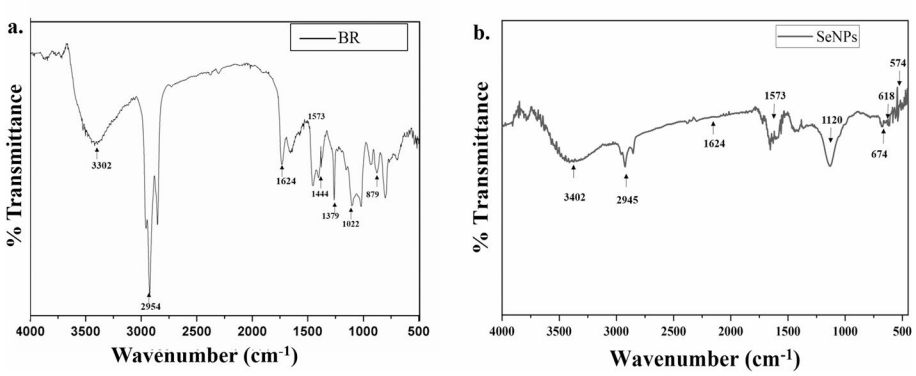

Fig. 6 Analysis of components associated with BR and SeNPs. **a** FTIR scan of BR; **b** FTIR scan of SeNPs

presence of different individual components such as C_{30}, C_{40}, and C_{50} isoprenoid derivatives of the pigment contributing to antioxidant mechanism reactions. Similar results were also observed by Nagar et al. [69] for methanolic pigment extract from three haloarchaea genera. They observed bands at 3305, 2972, 2926, 2879, 1444, 1379, 1087, 1047 and 879 cm^{-1}. These peaks corresponded to long chain groups, OH, C–O–C stretching vibrations, and C–H bending vibrations, indicating the presence of bacterioruberin. In the present study, the proposed mechanism of interaction of BR and As (III) is purely hypothetical and is attributed to a radical mechanism wherein H^+ donated by bacterioruberin may be involved in the reduction of toxic As (III) to stable As (0).

As seen in Fig. 6b, the FT-IR spectrum of the biologically synthesized SeNPs showed peaks at 3402, 2945, 1624, 1573, and 1120 cm^{-1}. The presence of these peaks, clearly indicated and confirmed the presence of biomacromolecules that have been absorbed onto the Se^0 particles and are now acting as capping agents. Broad peaks in 3402 cm^{-1} arose due to the stretching of the N–H bonds of amine (–NH) groups and the O–H bonds of the hydroxyl (–OH) groups. The absorption peaks at 2945 cm^{-1} featured the asymmetric stretching and bending vibrations of the C–H bond of the $–CH_2$ and CH_3 groups. The peak at 1624 and 1573 cm^{-1} is attributed to amide I & II in proteins. The absorption at 1120 cm^{-1} was typical of functional groups arising from polysaccharides. The peak at 574 cm^{-1} corresponded to the C–H group. This suggested the involvement of biomolecules such as pigment, proteins, peptides, amino acids, and aldehyde in the reduction of selenite to selenium and usually found as a capping agent at the surface of SeNPs as previously reported [62–64]. The involvement of these biomolecules in the reduction of selenite to selenium during growth has been confirmed previously in this same strain [47]. Further, the participation of such biomolecules in the reduction process and providing colloidal stability to other nanoparticles produced by this strain has been documented in earlier reports [48, 52].

3.7 Growth of GUSF-1 in the presence of arsenic and the role of pigment

Haloferax alexandrinus GUSF-1 grew as an orange-red culture, optimally in NTYE, pH 7, without a lag, and reached the stationary phase on day 5, with an absorbance of 1.834 monitored at 600 nm. The growth in the presence of 5 µM and 10 µM of As (III) was delayed by 2 days and was without any visible pigmentation with maximum absorbance of 0.822 and 0.49, respectively on day 5. Growth achieved in the absence of As (III) was 55.14% and 73.29% more than to that recorded for the culture growing in the presence

of 5 µM and 10 µM of As (III), respectively (Fig. 7). It is important to note that, despite delayed growth in the presence of 5 µM and 10 µM of As (III), the strain GUSF-1 continued its growth, tolerating both concentrations and proving its potential as an indicator of bioremediation. Secondly, although GUSF-1 was not able to endure high concentrations of arsenic as reported for *Haloferax mediterranei* (12 mM) belonging to the same genera [34], GUSF-1 maintained considerable growth and tolerance to the used arsenic concentration at high salt concentration (25% NaCl). Overall, in accordance with the results of the current experiment, we hypothesized that, the tolerance of GUSF-1 to 5 µM and 10 µM arsenic may be attributed to the cell-membrane C_{50} carotenoids (BR). Herein, we hypothesized that, during growth and cellular metabolism by culture in NTYE complex medium containing arsenic, BR may first interact with arsenite through ionic interaction activating electron transfer radical mechanisms transforming As (III) to As (0) thereby alleviating arsenic toxicity and promote growth. Further, the resistance of this strain to arsenic could be due to the presence of arsenite and arsenate resistance genes in their genome and megaplasmid as reported previously in haloarchaea [36–39]. For instance, arsenic detoxification was predicted in model haloarchaeon *Halobacterium* NRC-1 through arsenite biomethylation and the presence of metallochaperone, the product of *the arsD* gene, by Wang et al. [39]. In another study, arsenate respiration and arsenite oxidation genes were detected in eleven haloarchaeal isolates obtained from the red biofilm of Diamante Lake and the microbial mat of Tebenquiche Lake using metagenomics [36]. Tavossi et al. [28] studied the tolerance of 169 haloarchaeal isolates retrieved from saline and hypersaline habitats of Iran against heavy metal/oxyanions such as arsenate, cadmium, zinc, chromate, lead, mercury, copper, and selenite. Matarredona et al. [34] recently reported minimum inhibitory concentration of 12 mM arsenic for *Haloferax mediterranei* and *Halorubrum Californiense.*

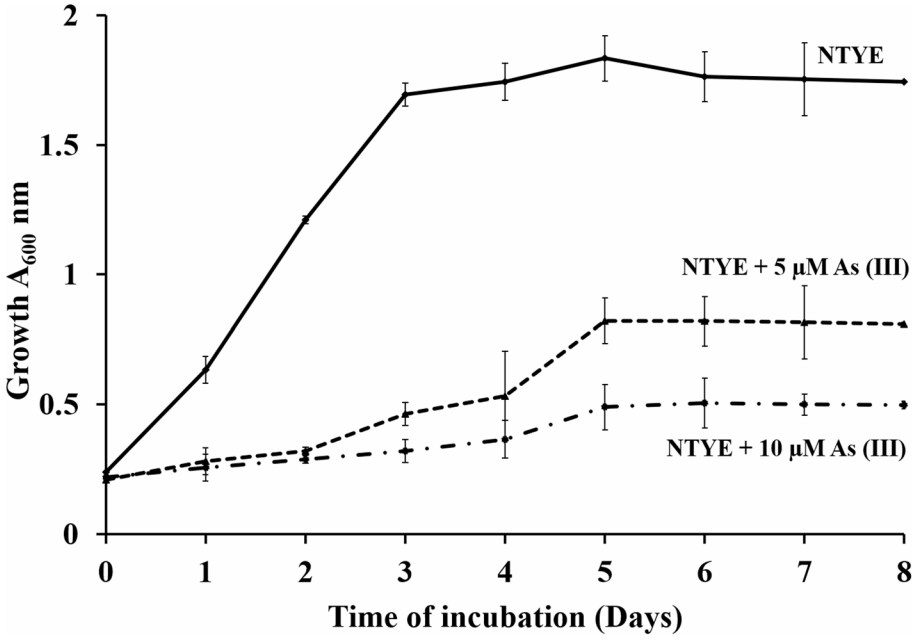

Fig. 7 Growth behavior of *Haloferax alexandrinus* GUSF-1 in NTYE in the absence and presence of 5 µM As (III) and 10 µM As (III)

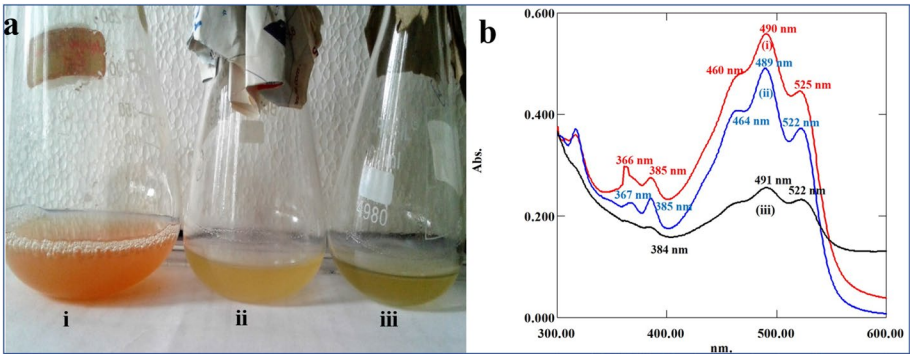

Fig. 8 Pigment analysis in the presence of arsenic during growth. **a**, Pigment production by *Haloferax alexandrinus* GUSF-1 in complex medium with and without arsenic; (i) NTYE; (ii) NTYE and 5 µM As (III) and (iii) NTYE and 10 µM As (III); **b**, Scan of extracted pigment from the cells of *Haloferax alexandrinus* GUSF-1 grown in NTYE (i), NTYE and 5 µM As (III) (ii) and NTYE and 10 µM As (III) (iii)

3.8 Pigment analysis of GUSF-1 grown in the presence of arsenic

In the absence of arsenic, GUSF-1 produced bright orange red pigment which showed peaks at 525 nm, 490 nm, 460 nm, 385 nm and 366 nm corresponding to absorbance of 0.446, 0.559, 0.473, 0.275 and 0.297, respectively (Fig. 8). These characteristics of three finger peaks indicated the presence of red C_{50} carotenoids in haloarchaea, especially the dominant bacterioruberin [46]. Surprisingly, spectroscopic scans of the methanolic extracts of cellular pigment grown in the presence of both concentrations of As (III) showed the characteristic peaks in the range from 300 to 600 nm. However, in the presence of 5 µM and 10 µM As (III), GUSF-1 produced light orange-red to light orange-yellow pigment, with shifts in the peak and reduced intensity (Fig. 8). For instance, in the presence of 5 µM As (III), pigment exhibited peaks at 522 nm, 489 nm, 464 nm, 385 nm and 367 nm corresponding to absorbance of 0.373, 0.490, 0.408, 0.234 and 0.226, respectively. While, pigment produced by strain in the presence of 10 µM As (III) showed only three peaks at 522 nm, 491 nm and 384 nm corresponding to the absorbance of 0.232, 0.256 and 0.178, respectively. These observations may reflect the ability of *Haloferax alexandrinus* GUSF-1 to avert the toxicity of 5 µM and 10 µM As (III), through its characteristic dominant C_{50} pigment component (bacterioruberin) in the cell-membrane.

Previous study by Wang et al. [76] showed that low concentrations of arsenic increased the growth of *Microcystis aeruginosa* cells, with little effect on pigment content. In addition, the high arsenite concentration specifically sensitive to chlorophyll a without affecting total carotenoid production. Baati et al. [31] reported varying degree of tolerance of *Halobacterium salinarum* to different concentration of metals such as Cd, Pb, Zn, Ni and Cu in complex and minimal media with decreased growth and pigmentation with increasing metal concentrations. Further, they speculated inhibition of pigment synthesizing enzyme or reduced growth can result in overall decrease in pigment production. Giani and Martinez-Espinosa [77] reported maximum bacterioruberin synthesis under oxidative stress, for example in the presence of H_2O_2. Their study highlighted the tolerance of H_2O_2 up to 25 mM above which there is reduced growth and therefore decreased cellular pigmentation. Generally, the pigment synthesis in haloarchaea is largely regulated by salinity, oxygen, light and pH [77]. Draft genome of five haloarchaeal strains belong to *H. salinarum* revealed the presence of genes responsible of metal resistance/transport, secondary metabolites and detoxification enzymes. The study documented

accumulation of carotenoids within the cell membrane as one of the tolerance strategies towards heavy metals (Cd, Pb, Zn, Ni and Cu). Further they hypothesized the tolerance of the strains to other heavy metals such As, Fe, Mo and Co [32]. Similar results on growth and pigment production in the presence of heavy metals [30, 78, 79] and aromatic pollutant [80] are documented in previous studies in haloarchaea retrieved from estuarine sediments and salt pans of Goa and India. Although these studies widely document the tolerance of haloarchaea to arsenic, the involvement of the haloarchaeal pigment and its components is not reported. In this context, GUSF-1 can be proposed as a promising bioremediation candidate for arsenic-contaminated saline waters, which can be made possible through its C_{50} red carotenoids.

4 Conclusion

Overall, the present study significantly adds to our understanding concerning the arsenic tolerance in *Haloferax alexandrinus* GUSF-1 and highlights the role of this haloarchaeon in arsenic bioremediation along with the potential use of BR and synthesized SeNPs in ameliorating arsenic toxicity in human cells. These results mark an initiating point to assess the role of BR and SeNPs from haloarchaea to alleviate As (III) toxicity, thus opening new avenues of research on haloarchaea in this significant field. While a detailed study on the mechanism and pharma-kinetics of BR and SeNPs for the amelioration of genotoxicity towards As (III) would be a desired outcome, the present study could find importance in the development of pharmaceuticals using extremely halophilic haloarcheon *Haloferax alexandrinus* GUSF-1(KF796625).

Supplementary Information

The online version contains supplementary material available at https://doi.org/10.1007/s42452-025-07602-0.

Supplementary Material 1

Supplementary Material 2

Acknowledgements

The author SG is grateful to Principal, Prof. Vikas J. Pissurlekar, and Prof. Sunita Borkar, M.Sc. Microbiology Coordinator, P.E. S's R.S.N. College of Arts and Science, Farmagudi, Ponda-Goa, for providing all the necessary lab facilities to carry out the research work on biological activities of BR and SeNPs. Additionally, the author SG acknowledges Department of Biotechnology, Ministry of Science and Technology, India for the grants provided under the DBT Star College Scheme Programme (HRD-11011/9/2023-HRD-DBT dated 08-11-2023). Authors acknowledge Dr. Maria Jose Wiseman Pinto, Professor and Head, Department of Microbiology, Goa Medical College, Bambolim, Goa, India, for the microbial pathogens used in the study.

Author contributions

Authors IF and JA designed the experiments. JJA carried out all the experimental benchwork for synthesizing BR and SeNPs. SG conducted antioxidant and antimicrobial activities of the prepared BR and SeNPs and provided critical feedback. AD performed and analyzed the Comet assay to determine the toxicity of As (III) on human lymphocytes. SKS analyzed the results of the Comet assay. SG critically analyzed the observations and results and formulated the MS along with JA.

Funding

The authors received no funding for conducting this study.

Data availability

Data is provided within the manuscript and supplementary information.

Declarations

Ethics approval and consent to participate

Goa University Institutional Human Ethics Committee (GU-IHEC) has waived off the need for ethical approval for the study because it involved routine research work procedures. Goa University Institutional Human Ethics Committee (GU-IHEC) waived the need for informed consent because of the routine research study.

Consent for publication
Not applicable.

Competing interests
The authors declare no competing interests.

Received: 25 October 2024 / Accepted: 7 August 2025
Published online: 12 August 2025

References

1. Shaji E, Santosh M, Sarath KV, Prakash P, Deepchand V, Divya BV. Arsenic contamination of groundwater: a global synopsis with focus on the Indian Peninsula. Geosci Front. 2021;1(3):101079. https://doi.org/10.1016/j.gsf.2020.08.015.
2. McArthur JM. Arsenic in groundwater. In: Sikdar P, editor. K, editor. Groundwater development and management. Cham: Springer; 2019. p. 279–308.
3. De Francisco P, Martín-González A, Rodriguez-Martín D, Díaz S. Interactions with arsenic: mechanisms of toxicity and cellular resistance in eukaryotic microorganisms. Int J Environ Res Public Health. 2021;18(22):12226.
4. Hajalilou B, Mosaferi M, Khaleghi F, Jadidi S, Vosugh B, Fatehifar E. Effects of abandoned arsenic mine on water resources pollution in North West of Iran. Health Promot Perspect. 2011;1(1):62–70. https://doi.org/10.5681/hpp.2011.006.
5. Nair M, Joseph T, Balachandran KK, Nair KKC, Paimpillii JS. Arsenic enrichment in estuarine sediments-impact of iron and manganese mining. Fate of arsenic in the environment. In: Ahmed MF, Ali MA, Adeel Z, editors International Symposium on Fate of Arsenic in the Environment; Dhaka; Bangladesh. International Training Network (ITN); Dhaka; Bangladesh. 2003. p. 57–67.
6. Fondekar SP, Reddy CVG. Arsenic content in the coastal and estuarine waters around Goa. Mahasagar Bull Nat Inst Ocean. 1974;7:27.
7. Zingde MD, Singbal SYS, Moraes CF, Reddy CVG. Arsenic, copper, zinc and manganese in the marine flora and fauna of coastal and estuarine waters around Goa. Indian J Mar Sci. 1976;5:212–7.
8. Zingde MD, Singbal SYS, Moraes CF, Reddy CVG. Some observations on pollutants of Velsao Bay (Goa). Mahasagar Bull Nat Inst Ocean. 1979;12(2):69–74.
9. Cantoni O, Zito E, Guidarelli A, Fiorani M, Ghezzi P. Mitochondrial ROS, ER stress, and Nrf2 crosstalk in the regulation of mitochondrial apoptosis induced by arsenite. Antioxidants. 2022;11(5):1034. https://doi.org/10.3390/antiox11051034.
10. de Boer J, Hoeijmakers JH. Nucleotide excision repair and human syndromes. Carcinogenesis. 2000;21(3):453–60. https://doi.org/10.1093/carcin/21.3.453.
11. Simeonova PP, Luster MI. Mechanisms of arsenic carcinogenicity: Genetic or epigenetic mechanisms? J Environ Pathol Toxicol Oncol. 2000;19(3):281–6.
12. Witkiewicz-Kucharczyk A, Bal W. Damage of zinc fingers in DNA repair proteins, a novel molecular mechanism in carcinogenesis. Toxicol Lett. 2006;162:29–42. https://doi.org/10.1016/j.toxlet.2005.10.018.
13. Hughes MF. Arsenic toxicity and potential mechanisms of action. Toxicol Lett. 2002;133(1):1–16. https://doi.org/10.1016/s0378-4274(02)00084-x.
14. Jasso-Pineda Y, Díaz-Barriga F, Calderón J, Yáñez L, Carrizales L, Pérez-Maldonado IN. DNA damage and decreased DNA repair in peripheral blood mononuclear cells in individuals exposed to arsenic and lead in a mining site. Biol Trace Elem Res. 2012;146(2):141–9. https://doi.org/10.1007/s12011-011-9237-0.
15. Vuyyuri SB, Ishaq M, Kuppala D, Grover P, Ahuja YR. Evaluation of micronucleus frequencies and DNA damage in glass workers exposed to arsenic. Environ Mol Mutagen. 2006;47(7):562–70. https://doi.org/10.1002/em.20229.
16. Yáñez L, García-Nieto E, Rojas E, Carrizales L, Mejía J, Razo I, Díaz-Barriga F. DNA damage in blood cells from children exposed to arsenic and lead in a mining area. Environ Res. 2003;93(3):231–40. https://doi.org/10.1016/j.envres.2003.07.005.
17. Ladeira C, Møller P, Giovannelli L, Gajski G, Haveric A, Bankoglu EE, Collins A. The comet assay as a tool in human biomonitoring studies of environmental and occupational exposure to Chemicals—a systematic scoping review. Toxics. 2024;12(4):270.
18. Anderson P, Kedersha N. Stress granules. Curr Biol. 2009;19(10):397–8. https://doi.org/10.1016/j.cub.2009.03.013.
19. Coelho DG, de Andrade HM, Marinato CS, Araujo SC, de Matos LP, da Silva VM, de Oliveira JA. Exogenous jasmonic acid enhances oxidative protection of *Lemna Valdiviana* subjected to arsenic. Acta Physiol Plant. 2020;42:97.
20. Lee X, Weinfeld M. Cellular response to arsenic: DNA damage and defense mechanisms. London (UK): IWA Publishing; 2004.
21. Ventura-Lima J, Bogo MR, Monserrat JM. Arsenic toxicity in mammals and aquatic animals: a comparative biochemical approach. Ecotoxicol Environ Saf. 2011;74(3):211–8. https://doi.org/10.1016/j.ecoenv.2010.11.002.
22. Vineetha RC, Binu P, Arathi P, Nair RH. L-ascorbic acid and α-tocopherol attenuate arsenic trioxide-induced toxicity in H9c2 cardiomyocytes by the activation of Nrf2 and Bcl2 transcription factors. Toxicol Mech Methods. 2018;28(5):353–60. https://doi.org/10.1080/15376516.2017.1422578.
23. William VU, Magpantay HD. Arsenic and microorganisms: genes, molecular mechanisms, and recent advances in microbial arsenic bioremediation. Microorganisms. 2023;12(1):74.
24. Cui H-L, et al. Proposed minimal standards for description of new taxa of the class *Halobacteria*. Int J Syst Evol Microbiol. 2024;74:006290.
25. Oren A. Halophilic archaea on Earth and in space: growth and survival under extreme conditions. Philos Trans R Soc A-Math Phys Eng Sci. 2014;372:20140194.
26. Voica DM, Bartha L, Banciu HL, Oren A. Heavy metal resistance in halophilic bacteria and archaea. FEMS Microbiol Lett. 2016;363(14):fnw146.
27. Srivastava P, Kowshik M. Mechanisms of metal resistance and homeostasis in Haloarchaea. Archaea. 2013;2013(1):732864.
28. Tavoosi N, Sepahi A, Amoozegar A, M. A., and, Kiarostami V. Toxic heavy metal/oxyanion tolerance in Haloarchaea from some saline and hypersaline ecosystems. J Basic Microbiol. 2023;63(5):558–69.

29. Vera-Bernal M, Martínez-Espinosa RM. Insights on cadmium removal by bioremediation: the case of Haloarchaea. Microbiol Res. 2021;12(2):354–75.
30. Das D, Salgaonkar BB, Mani K, Braganca JM. Cadmium resistance in extremely halophilic archaeon *Haloferax* strain BBK2. Chemosphere. 2014;112:385–92.
31. Baati H, Siala M, Azri C, Ammar E, Dunlap C, Trigui M. Resistance of a *Halobacterium salinarum* isolate from a solar saltern to cadmium, lead, nickel, zinc, and copper. Antonie Van Leeuwenhoek. 2020;113:1699–711.
32. Baati H, Siala M, Azri C, Ammar E, Dunlap C, Trigui M. Genomic analysis of heavy metal-resistant *Halobacterium salinarum* isolated from Sfax solar saltern sediments. Extremophiles. 2022;26(2):25.
33. Baati H, Siala M, Benali S, Azri C, Dunlap C, Martínez-Espinosa RM, Trigui M. Elucidating metabolic pathways through genomic analysis in highly heavy metal-resistant *Halobacterium salinarum* strains. Heliyon. 2024;10(23).
34. Matarredona L, Zafrilla B, Camacho M, Bonete MJ, Esclapez J. Understanding the tolerance of halophilic archaea to stress landscapes. Environ Microbiol Rep. 2024;16(6):e70039.
35. Straková D, Sánchez-Porro C, de la Haba RR, Ventosa A. Strategies of environmental adaptation in the haloarchaeal genera *Haloarcula* and *Natrinema*. Microorganisms. 2025;13(4):761.
36. Ordoñez OF, Rasuk MC, Soria MN, Contreras M, Farías ME. Haloarchaea from the Andean puna: biological role in the energy metabolism of arsenic. Microb Ecol. 2018;76:695–705.
37. Rascovan N, Maldonado J, Vazquez MP, Eugenia Farías M. Metagenomic study of red biofilms from diamante lake reveals ancient arsenic bioenergetics in Haloarchaea. ISME J. 2016;10(2):299–309.
38. Taran M, Monaza A, Zavar J, Safari M, Bakhtiyari S. Optimal conditions for the biological removal of arsenic by a novel halophilic archaea in different conditions and its process optimization. Pol J Chem Tech. 2013;15(2):7–9. https://doi.org/10.2478/pjct-2013-0017.
39. Wang G, Kennedy SP, Fasiludeen S, Rensing C, DasSarma. S. Arsenic resistance in *Halobacterium* sp. strain NRC-1 examined by using an improved gene knockout system. J Bacteriol. 2004;186(10):3187–94. https://doi.org/10.1128/JB.186.10.3187-3194.2004.
40. Moopantakath J, Imchen M, Anju VT, Busi S, Dyavaiah M, Martínez-Espinosa RM, Kumavath R. Bioactive molecules from haloarchaea: scope and prospects for industrial and therapeutic applications. Front Microbiol. 2023;14:1113540.
41. Giani M, Pire C, Martínez-Espinosa RM. Bacterioruberin: biosynthesis, antioxidant activity, and therapeutic applications in cancer and immune pathologies. Mar Drugs. 2024;22(4):167.
42. Serrano S, Mendo S, Caetano T. Haloarchaea have a high genomic diversity for the biosynthesis of carotenoids of biotechnological interest. Res Microbiol. 2022;173(3):103919.
43. Khandavilli S, Sequiera F, Furtado I. Ecol Environ Conserv. 1999;5:149.
44. Naik-Samant S, Gaonkar S, Furtado I. Bio-adsorption of Fe (II) by dry biomass of metal-tolerant Haloarchaeon *Haloferax Alexandrinus* GUSF-1. Braz J Microbiol. 2024;1–14.
45. Alvares JJ, Furtado IJ. Kinetics of DPPH$^{\bullet}$ scavenging by Bacterioruberin from *Haloferax Alexandrinus* GUSF-1 (KF796625). J Anal Sci Tech. 2021b;12:44. https://doi.org/10.1186/s40543-021-00293-3.
46. Alvares JJ, Furtado IJ. Characterization of multicomponent antioxidants from *Haloferax Alexandrinus* GUSF-1 (KF796625). 3 biotech. 2021;11:58. https://doi.org/10.1007/s13205-020-02584-9
47. Alvares JJ, Furtado IJ. Conversion of selenite by *Haloferax Alexandrinus* GUSF-1(KF796625) to pentagonal selenium nanoforms which in vitro modulates the formation of calcium oxalate crystals. J Appl Microbiol. 2022;132(3):1900–13. https://doi.org/10.1111/jam.15309.
48. Alvares JJ, Furtado IJ. Anti-*Pseudomonas aeruginosa* biofilm activity of tellurium nanorods biosynthesized by cell lysate of *Haloferax Alexandrinus* GUSF-1(KF796625). Biometals. 2021a;34(5):1007–16. https://doi.org/10.1007/s10534-021-00323-y.
49. Naik-Samant S, Furtado IJ. Biomineralization of Fe^{3+} to nanosized γFe_2O_3 by *Haloferax Alexandrinus* GUSF-1. Geomicrobiol J. 2021;38(9):809–15. https://doi.org/10.1080/01490451.2021.1954730.
50. Naik-Samant S, Furtado I. Formation of rhodochrosite by *Haloferax Alexandrinus* GUSF-1. J Cluster Sci. 2019;30:1435–41. https://doi.org/10.1007/s10876-019-01586-9.
51. Alvares JJ, Gaonkar SK, Naik CC, Asogekar P, Furtado IJ. Characterization of Mn_3O_4-MnO_2 nanocomposites biosynthesized by cell lysate of *Haloferax Alexandrinus* GUSF-1. J Basic Microbiol. 2023;63(9):996–1006. https://doi.org/10.1002/jobm.202300023.
52. Patil S, Fernandes J, Tangsali RB, Furtado I. Exploitation of *Haloferax Alexandrinus* for biogenic synthesis of silver nanoparticles antagonistic to human and lower mammalian pathogens. J Clust Sci. 2014;25:423–33. https://doi.org/10.1007/s10876-013-0621-0.
53. Li S, Dong X, Xu L, Wu Z. Nephroprotective effects of selenium nanoparticles against sodium Arsenite-Induced damages. Int J Nanomed. 2023;13:18:3157–76. https://doi.org/10.2147/IJN.S413362. PMID: 37333733; PMCID: PMC10276609.
54. Prasad KS, Selvaraj K. Biogenic synthesis of selenium nanoparticles and their effect on as (III)-induced toxicity on human lymphocytes. Biol Trace Elem Res. 2014;157(3):275–83. https://doi.org/10.1007/s12011-014-9891-0.
55. Bjørklund G, Rahaman MS, Shanaida M, Lysiuk R, Oliynyk P, Lenchyk L, Peana M. Natural dietary compounds in the treatment of arsenic toxicity. Molecules. 2022;27(15):4871.
56. Das R, Das A, Roy A, Kumari U, Bhattacharya S, Haldar PK. beta-Carotene ameliorates arsenic-induced toxicity in albino mice. Biol Trace Elem Res. 2015;164:226–33.
57. Gaonkar SK, Furtado IJ. Isolation and culturing of protease-and lipase-producing *Halococcus agarilyticus* GUGFAWS-3 from marine *Haliclona* sp. inhabiting the Rocky intertidal region of anjuna in goa, India. Ann Microbiol. 2018;68:851–61. https://doi.org/10.1007/s13213-018-1391-6.
58. Sahli K, Gomri MA, Esclapez J, Gómez-Villegas P, Ghennai O, Bonete MJ, Kharroub K. Bioprospecting and characterization of pigmented halophilic archaeal strains from Algerian hypersaline environments with analysis of carotenoids produced by *Halorubrum* sp. BS2. J Basic Microbiol. 2020;60(7):624–38.
59. Strober W. Trypan blue exclusion test of cell viability. Curr Protoc Immunol. 2015;111:A3.B.1–3. https://doi.org/10.1002/0471142735.ima03bs111.
60. Dhawan A, Mathur N, Seth PK. The effect of smoking and eating habits on DNA damage in Indian population as measured in the comet assay. Mutat Res. 2001;474(1–2):121 – 28. https://doi.org/10.1016/s0027-5107(00)00171-8.
61. Konca K, Lankoff A, Banasik A, Lisowska H, Kuszewski T, Gozdz S, Koza Z, Wojcik A. Cross-platform public domain PC image-analysis program for the comet assay. Mutat Res. 2003;534(1–2):15–20. https://doi.org/10.1016/s1383-5718(02)00251-6.

62. Abdollahnia M, Makhdoumi A, Mashreghi M, Eshghi H. Exploring the potentials of halophilic prokaryotes from a solar saltern for synthesizing nanoparticles: the case of silver and selenium. PLoS One. 2020;15(3):e0229886. https://doi.org/10.1371/journal.pone.0229886.
63. Srivastava P, Bragança JM, Kowshik M. In vivo synthesis of selenium nanoparticles by *Halococcus Salifodinae* BK18 and their anti-proliferative properties against HeLa cell line. Biotechnol Prog. 2014;30(6):1480–7. https://doi.org/10.1002/btpr.1992.
64. Nagar DN, Ghosh NN, Braganca JM. Green synthesis of selenium nanospheres and nanoneedles by halophilic archaea. Appl Nanosci. 2022;12(12):3983–94.
65. Sahli K, Gomri MA, Esclapez J, Gómez-Villegas P, Bonete MJ, León R, Kharroub K. Characterization and biological activities of carotenoids produced by three haloarchaeal strains isolated from Algerian salt lakes. Arch Microbiol. 2022;204(1):6.
66. Serov DA, Khabatova VV, Vodeneev V, Li R, Gudkov SV. A review of the antibacterial, fungicidal and antiviral properties of selenium nanoparticles. Materials. 2023;16(15):5363.
67. Huang D, Ou B, Prior RL. The chemistry behind antioxidant capacity assays. J Agric Food Chem. 2005;53(6):1841–56. https://doi.org/10.1021/jf030723c.
68. Hou J, Cui HL. In vitro antioxidant, antihemolytic, and anticancer activity of the carotenoids from halophilic archaea. Curr Microbiol. 2018;75(3):266–71. https://doi.org/10.1007/s00284-017-1374-z.
69. Nagar DN, Das D, Braganca JM. Antioxidant potential of pigments produced by halophilic archaea isolated from salt pans of India. Environ Sustain. 2024;1–9.
70. Bouhamed SBH, Chaari M, Baati H, Zouari S, Ammar E. Extreme halophilic archaea: *Halobacterium salinarum* carotenoids characterization and antioxidant properties. Heliyon 2024;10(17).
71. Kumaravel TS, Vilhar B, Faux SP, Jha AN. Comet assay measurements: a perspective. Cell Biol Toxicol. 2009;25(1):53–64. https://doi.org/10.1007/s10565-007-9043-9.
72. Shahmohammadi HR, Asgarani E, Terato H, Saito T, Ohyama Y, Gekko K, Yamamoto O, Ide H. Protective roles of Bacterioruberin and intracellular KCl in the resistance of *Halobacterium salinarium* against DNA-damaging agents. J Radiat Res. 1998;39(4):251–62. https://doi.org/10.1269/jrr.39.251.
73. Zwolak I. The role of selenium in arsenic and cadmium toxicity: an updated review of scientific literature. Biol Trace Elem Res. 2020;193(1):44–63. https://doi.org/10.1007/s12011-019-01691-w.
74. Chitta KR, Figueroa L, Caruso JA, J. A., Merino EJ. Selenium mediated arsenic toxicity modifies cytotoxicity, reactive oxygen species and phosphorylated proteins. Metallomics. 2013;5(6):673–85.
75. Rahman MM, Uson-Lopez RA, Sikder MT, Tan G, Hosokawa T, Saito T, Kurasaki M. Ameliorative effects of selenium on arsenic-induced cytotoxicity in PC12 cells via modulating autophagy/apoptosis. Chemosphere. 2018;196:453–66.
76. Wang S, Zhang D, Pan X. Effects of arsenic on growth and photosystem II (PSII) activity of *Microcystis aeruginosa*. Ecotoxicol Environ Saf. 2012;84:104–11.
77. Giani M, Martínez-Espinosa RM. Carotenoids as a protection mechanism against oxidative stress in *Haloferax mediterranei*. Antioxidants. 2020;9(11):1060.
78. Braganca JM, Furtado I. Resistance of *Halobacterium* strain R1 to cadmium during growth in mineral salts medium devoid of growth factors. Asian J Microbiol Biotech Environ Sci. 2013;15:299–302.
79. Salgaonkar BB, Das D, Bragança JM. Resistance of extremely halophilic archaea to zinc and zinc oxide nanoparticles. Appl Nanosci. 2016;6(2):251–8.
80. Raghavan T, Furtado M, I. Expression of carotenoid pigments of haloarchaeal cultures exposed to aniline. Environ Toxicol. 2005;20(2):165–9. https://doi.org/10.1002/tox.20091.

Publisher's note